CHEMICAL EVOLUTIONS OF GMCS WHILE CROSSING THE SPIRAL ARM IN THE NEARBY GALAXY M 83

Taku Sugiuchi, Kazuyuki Muraoka, Ryouhei Harada, Shota Takada, Aya Homma (Osaka Pref. Univ), Kazuki Tokuda (Osaka Pref. Univ. /NAOJ), Tomoka Tosaki (Jouetsu Univ. of Education), Junichi Baba , Akihiro Hirota , Fumi Egusa (NAOJ), Kotaro Kohno (IoA/UT), Kouichiro Nakanishi(NAOJ), Nario Kuno (Univ. of Tsukuba)

Abstract

We observed molecular lines including ^{13}CO(1-0), C^{18}O(1-0), CS(2-1), and CH_3OH(2-1) simultaneously toward the eastern spiral arm of M 83 in order to study the evolution of GMCs while crossing the spiral arm in terms of chemical properties in the ALMA Cycle-4. The field coverage is ~107" × 70". ^{13}CO(1-0) emission revealed the global distribution of molecular gas, and C^{18}O(1-0), CS(2-1), and CH_3OH(2-1) emissions are found in local peaks of ^{13}CO(1-0). C^{18}O/^{13}CO, CS/^{13}CO ratios tend to increase in the downstream side of the spiral arm. We have identified 32 clumps as GMCs based on *dendrogram* algorithm. We examined the correlations between size and velocity widths and between molecular gas mass (LTE mass) and virial mass for identified GMCs. These correlations are well consistent with those in earlier studies (e.g., Tosaki et al. 2017).

Introduction

Since Giant Molecular Clouds (GMCs) are major sites of massive star formation, it is important to study the evolution of GMCs in galaxies.

So far, GMC evolutions while crossing spiral arms have been studied by many investigators. Based on mm-wave interferometric observations, Egusa et al. (2011) and Hirota et al.(2011) revealed that massive clouds tend to be located in downstream side of the spiral arm and are virialized, associated with HII regions, while smaller clouds tends to be in upstream side and are less massive and unvirialized.

However, these studies are mostly based on the limited molecule, such as CO. It is also important to observe other molecular lines (e.g., Tosaki et al. 2017). For example, C^{18}O(1-0) and CS(2-1) emission are enhanced in dense gas/massive star forming regions while CH_3OH(2-1) is enhanced in spiral shock wave and is dissociated by intense UV radiation from massive stars.

Examining spatial variations in C^{18}O/^{13}CO, CS/^{13}CO and CH_3OH/^{13}CO ratios in the spiral arm enables us to investigate physical/chemical evolutions of GMCs in detail.

ALMA observations

Target : M 83

- grand-design barred spiral galaxy
- D = 4.5 Mpc (1″ = 22 pc ; Thim et al. 2003)
- face-on : i = 22

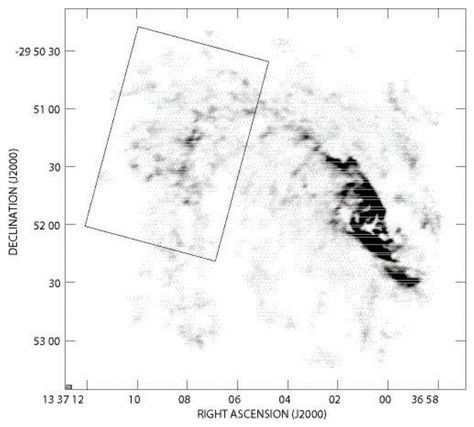

Fig. 1 : The target field (107" × 70" rectangle) for ALMA cycle-4 superposed on the ^{12}CO(1-0) intensity map.

Observation parameters

- Telescopes : ALMA 12-m Array
- Observed area : 107" × 70" rectangle (see Fig.1)
- Observed lines

line/transition	rest frequency (GHz)	Beam size (arcsec)	Position angle (degree)	rms noise level (mJy/beam (dv = 4km/s))
^{13}CO(J=1-0)	110.2014	2.11 × 1.72	-88.74	0.43
C^{18}O(J=1-0)	109.7822	2.12 × 1.62	-89.24	0.43
CS(J=2-1)	97.98095	2.38 × 1.81	-89.16	0.33
CH_3OH(J=2-1)	96.74138	2.42 × 1.82	-89.69	0.35

Results & Discussion

Integrated Intensity map

We compare ^{13}CO(1-0) integrated intensities (contours) with other emission (color).

The strong Hα emission is observed in the downstream side of ^{13}CO(1-0) arm rather than the upstream side. IRAC 8μm emission is well spatially coincident with the ^{13}CO(1-0) intensity.

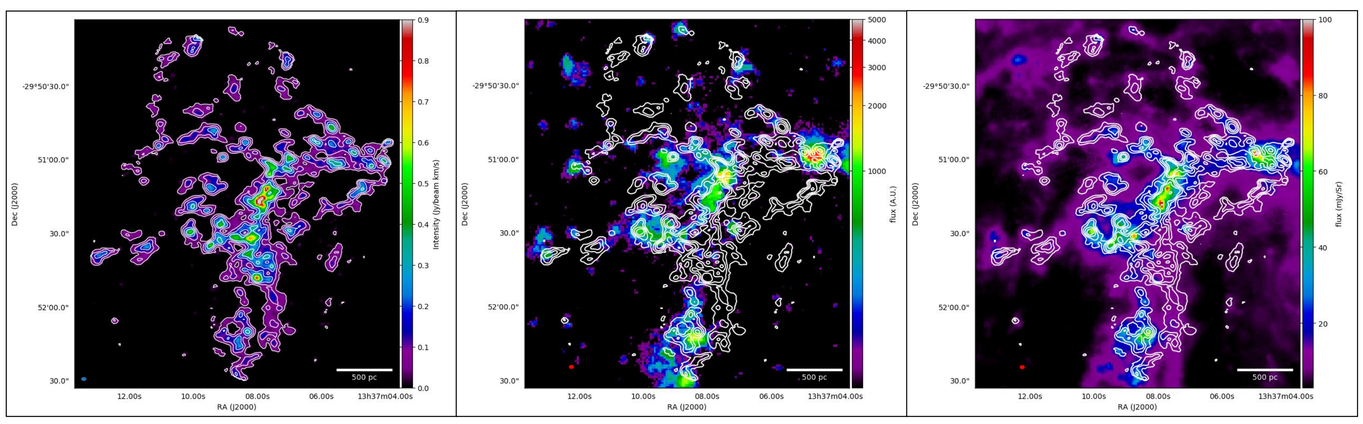

Fig. 3.1 : ^{13}CO(1-0) Fig. 3.2 : Hα Fig. 3.3 : IRAC 8μm

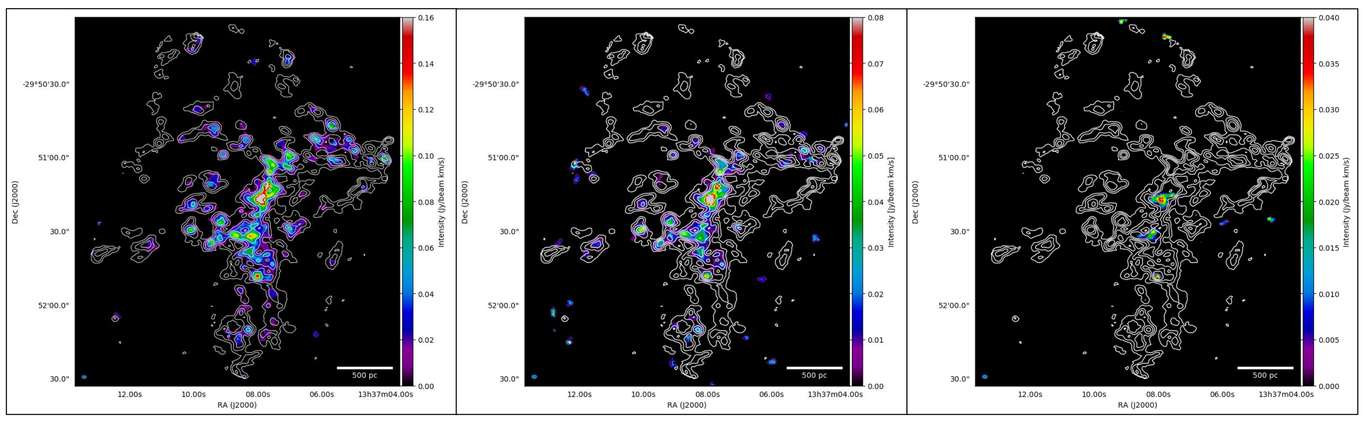

Fig. 3.4 : C^{18}O(1-0) Fig. 3.5 : CS(2-1) Fig. 3.6 : CH_3OH (2(0,2)-1(0,1))

Fig. 3 : Integrated intensity maps of ^{13}CO(1-0) emission (contours) superposed on other emission (color). The pixel size is 0".5. The contour levels are 60, 200, 400 and 700 σ where 1 σ = 0.43 mJy beam^{-1}.

Intensity Ratio Map

We examined spatial variations in C^{18}O(1-0)/^{13}CO(1-0), CS(2-1)/^{13}CO(1-0), and CH_3OH(2-1)/^{13}CO(1-0) ratios.

C^{18}O/^{13}CO, CS/^{13}CO ratios tend to increase in the downstream side of the spiral arm.

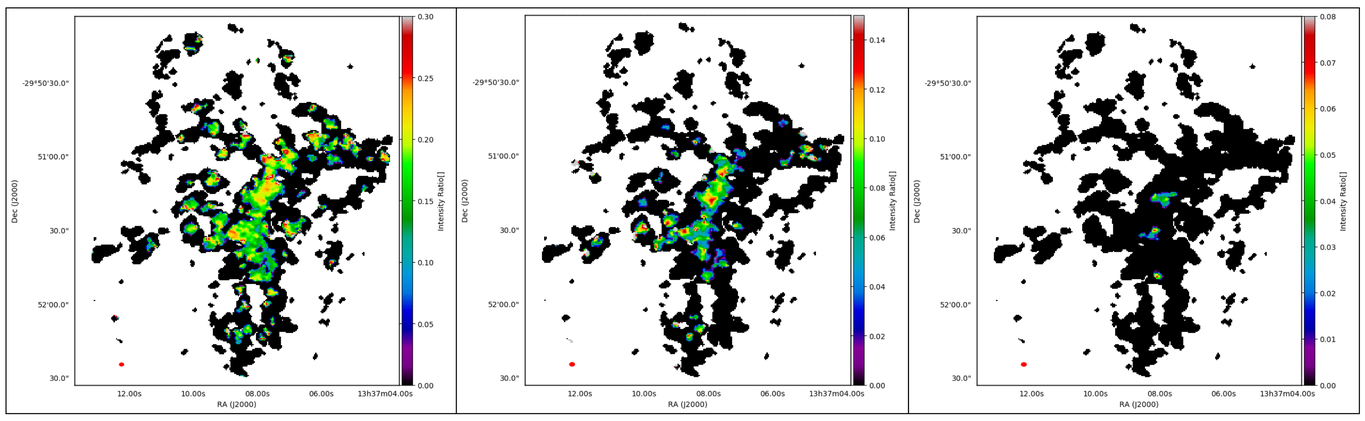

Fig. 4.1 : C^{18}O/^{13}CO Fig. 4.2 : CS/^{13}CO Fig. 4.3 : CH_3OH/^{13}CO

Cloud Identification We applied the *dendrogram* algorithm (Rosolowsky et al. 2008) to the ^{13}CO(1-0) data cube in order to decompose the ^{13}CO emission into discrete clouds and to measure their physical properties. This algorithm makes a tree that represents the hierarchy of the structures in the data. For example, large clouds are trunks, and small ones are leaves.

We have identified 32 clumps as GMCs(Fig. 5). For identified GMCs, we examined the size-velocity width relation of identified GMCs (Fig. 6) and correlation between LTE mass and virial mass of them(Fig. 7), using the following equations.

$$\underset{[M_\odot]}{M_{VIR}} = 210 \underset{[pc]}{R} (\underset{[km\ s^{-1}]}{\Delta v})^2$$

$$\underset{[cm^{-1}]}{N_{H_2}} = 2.41 \times 10^5 \times \frac{[H_2]}{[^{13}CO]} \frac{e^{5.29/T_{ex}}}{e^{5.29/T_{ex}} - 1} \times \underset{[K\ km\ s^{-1}]}{I_{^{13}CO}}$$

$$\underset{[M_\odot]}{M_{LTE}} = \underset{[cm^{-1}]}{N_{H_2}} \times \underset{[kg]}{\mu} \times \underset{[cm]}{pix^2} \times \underset{[M_\odot\ kg^{-1}]}{M_\odot / M_{H_2}}$$

assuming $\frac{[H_2]}{[^{13}CO]} = 5.0 \times 10^5$ (Dickman et al. 1978),

Excitation temperature : $T_{ex} = 20$ K

mean molecular weight per H_2 : μ = 2.8 kg

length per 1 pixel : *pix* = 1.6264 × 10^{19} cm

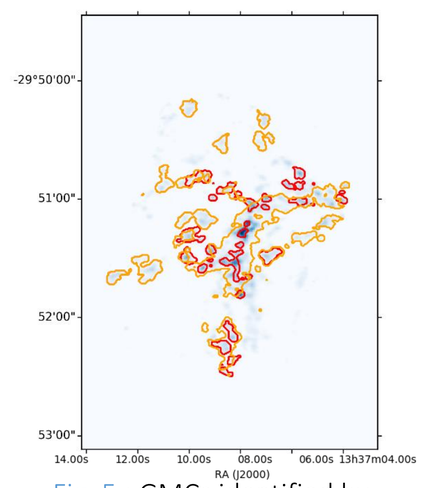

Fig. 5 : GMCs identified by *dendrogram*. Each red enclosure corresponds to a GMC.

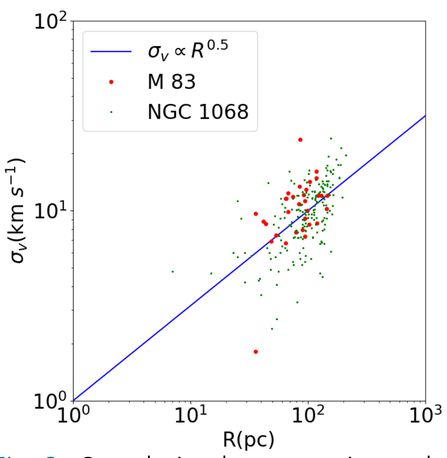

Fig. 6 : Correlation between size and velocity width of the identified GMCs in M83. The diagonal line indicates Larson's Law, $\sigma_V \propto R^{0.5}$(Larson 1981).

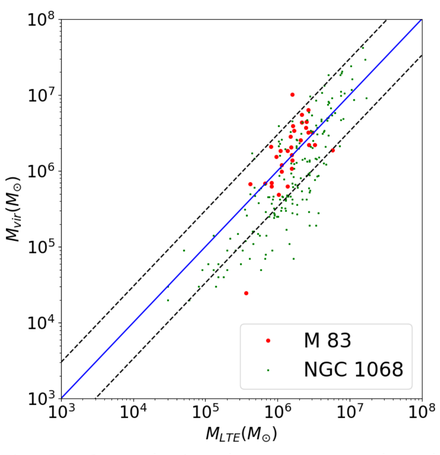

Fig. 7 : Correlation between molecular gas mass (LTE mass) and virial mass of the identified GMCs in M83. The diagonal line shows $M_{LTE} = M_{VIR}$

Future Works

- Deriving C^{18}O/^{13}CO, CS/^{13}CO and CH_3OH/^{13}CO ratios and virial parameters for each identified GMC.
- Investigating their variations according to upstream/downstream side of the spiral arm.
- Unveiling physical/chemical evolution of GMCs while crossing spiral arms.

References

・Egusa et al. 2011 Apj, 726, 85 ・Hirota et al. 2011, ApJ, 737, 40・Tosaki et al. 2017 PASJ, 69 18 ・Thim et al. 2003, ApJ, 590, 256 ・Rosolowsky et al. 2008, ApJ, 679, 1338-1351 ・Dickman, R. L. 1978, ApJS, 37, 407・Larson, R. B. 1981, MNRAS, 194, 809